Asian Journal of Chemistry; Vol. 33, No. 2 (2021), 359-366

ASIAN JOURNAL OF CHEMISTRY

https://doi.org/10.14233/ajchem.2021.23007

Syntheses, Structures, Magnetic Properties and Antibacterial Activities of Two Copper(II) Azido Complexes with Varied Nuclearities Containing Symmetrical 1,3-Diammine as Chelator

HABIBAR CHOWDHURY[1] and CHANDAN ADHIKARY[2,*]

[1]Department of Chemistry, Kabi Nazrul College, Murarai, Birbhum-731 219, India
[2]Department of Education, The University of Burdwan, Golapbag, Burdwan-713104, India

*Corresponding author: E-mail: cadhikary123@gmail.com

Received: 6 October 2020; *Accepted*: 20 November 2020; *Published online*: 15 January 2021; AJC-20221

Two copper(II) azido complexes of the types mononuclear $[Cu(TMEDA)_2(N_3)_2]$ (**1**) and dinuclear $[Cu(TMEDA)(\mu_{1,1}\text{-}N_3)(N_3)]_2$ (**2**) [TMEDA = trimethylenediamine; N_3^- = azide ion] have been synthesized and characterized. X-ray structural analysis revealed that each copper(II) center in complex **1** adopts a distorted octahedron geometry with a CuN_6 chromophore ligated through four N atoms of two different symmetrical TMEDA ligands as bidentate chelator and two N atoms of two terminal azides. In complex **2**, each copper(II) center adopts a distorted square pyramidal geometry with a CuN_5 chromophore ligated through two N atoms of TMEDA as bidentate chelator and two N atoms of two different azides as $\mu_{1,1}$-N_3 bridging mode and one N atom of terminal azide ion. The two copper centers are connected through double $\mu_{1,1}$-N_3 bridges affording a dinuclear structure with Cu···Cu separation 3.327(2) Å. In crystalline state, mononuclear units in complex **1** are associated through intermolecular N-H···N and C-H···N hydrogen bonds to form a 2D sheet structure viewed along crystallographic *b*-axis, whereas dinuclear entities in complex **2** are propagated through intermolecular N-H···N and C-H···N hydrogen bonds to form a 3D network structure viewed along crystallographic *a*-axis. The Variable-temperature magnetic susceptibility measurement evidenced a dominant antiferromagnetic interaction between the metal centers through $\mu_{1,1}$-azide bridges in complex **2** with $J = -0.40$ cm^{-1}. The antibacterial activities of the complexes have also been studied.

Keywords: Dinuclear, Copper(II) complex, Terminal azide, Bridged azide, X-ray structure, Antibacterial activities.

INTRODUCTION

Growth and developments of metal-organic frameworks (MOFs) [1] have enchanted research communities worldwide due to their amazing features and extensive applications [2-5]. These properties can be subdued by the sensible choice of metal ions, ligands and bridging moieties. One-pot synthesis [6] of the building units is one of the diligent strategies to sketch such topologies based on strong metal-ligand covalent interactions [7] and multiple weak non-covalent interactions like hydrogen bonds [8]. Copper(II), a $3d^9$ ion, delivers [9-11] a variety of geometries with different nuclearities and versatile pseudohalides bridges have evolved a great focus due to their impressive structures, catalytic and magnetic properties [12-17] and also as models for the active sites of biomolecules [18]. Symmetrical 1,2-diamine [19] is the significant blockers to synthesize coordination polymers of different dimensionalities. Homo atomic azide ions [20] are mostly employed because of its bridging versatilities yielding coordination compounds of comprehensive structures and functional variability. The conventional bridging modes (**Scheme-I**) of these pseudohalide are $\mu_{1,1}$ (end-on, EO) and $\mu_{1,3}$ (end-to-end, EE) yielding both ferromagnetic and antiferromagnetic coupling depending upon multiple factors between/among paramagnetic metal ions [21-27]. This work stems from our continuing interest to aggravate such investigation with azides in combination with an symmetrical bidentate amine, trimethylenediamine (TMEDA) to prepare mono-, di- or polynuclear copper(II) complexes. We have successfully synthesized and characterized one mononuclear copper(II) azido complex $[Cu(TMEDA)_2(N_3)_2]$ (**1**) and one dinuclear copper-(II)azido complex $[Cu(TMEDA)(\mu_{1,1}\text{-}N_3)(N_3)]_2$ (**2**) [TMEDA = trimethylenediamine; N_3^- = azide ion]. This study has addressed the details of syntheses, characterizations, X-ray structures, magnetic property and antibacterial activities of two complexes.

This is an open access journal, and articles are distributed under the terms of the Attribution 4.0 International (CC BY 4.0) License. This license lets others distribute, remix, tweak, and build upon your work, even commercially, as long as they credit the author for the original creation. You must give appropriate credit, provide a link to the license, and indicate if changes were made.

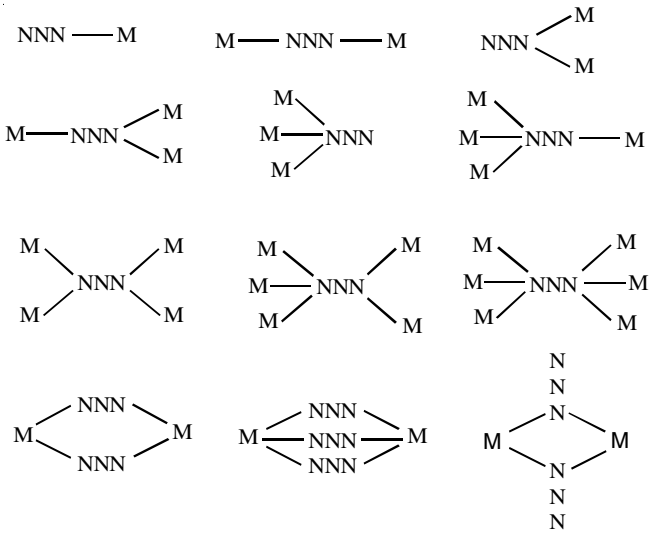

Scheme-I: Possible coordination motifs of azide ion

EXPERIMENTAL

High purity trimethylenediamine (Sigma-Aldrich, USA), sodium azide (Sigma-Aldrich, USA) and copper(II) chloride dihydrate (E. Merck, India) were purchased from their respective concerns and used as received. All other chemicals and solvents were of AR grade and were distilled and dried before use. The synthetic reactions and work-up were done in the open atmosphere.

Caution! Azido complexes of transition metal ions are potentially explosive, especially in the presence of organic ligands. Only a little amount of the materials should be prepared and handled with proper care.

Elemental analyses (carbon, hydrogen and nitrogen) were performed on a Perkin-Elmer 240C elemental analyzer. The IR spectrum (KBr disc, 4000-200 cm^{-1}) was recorded using a Nicolate Magna IR 750 Series II FTIR spectrometer. Ground state absorption (in methanol) was measured with a Perkin Elmer LAMBDA EZ-301 spectrophotometer. Variable-temperature (1.8-300 K) magnetic measurements were carried out using a Quantum Design SQUID-based MPMSXL-5-type magnetometer. The palladium rod sample (Materials Research Corporation, measured purity 99.9985%) was used to calibrate the SQUID magnetometer where the superconducting magnet was normally run from 0 to 5 T field strength. Measurements were made at a magnetic field of 0.5 T. Corrections are based on subtracting the sample holder signal and contribution χ_D estimated from the Pascal constants [28]. Magnetization measurements were conducted at 2 K in the magnetic field from 0 to 5 T. X-band (9.5 GHz) EPR measurements were done on polycrystalline samples using a Bruker ElexSys E 500 spectrometer. The measurements were performed at room and liquid nitrogen temperature. The spectrometer was equipped with NMR teslameter (ER 036TM) and at X-band frequency counter (E 41 FC). Measurements parameters were as follows: microwave power 10 mW, modulation amplitude 8 G, centre field 3500 G, range 7000 G for X-band.

Synthesis of $[Cu(TMEDA)_2(N_3)_2]$ (1): To a methanolic solution (15 mL) of copper(II) chloride dihydrate (0.170 g, 1 mmol), TMEDA (0.340 g, 2 mmol) was added. Then sodium azide (0.130 g, 2 mmol) dissolved in MeOH (10 mL) was added dropwise with constant stirring the mixture for about 20 min. The above mixture was heated with stirring for about 30 min and then filtered when it was still hot. After filtration through a fine glass-frit, the supernatant green solution was kept in air for slow evaporation. Deep blue coloured single crystals of **1** were deposited within a week, which were separated by filtration and dried *in vacuo* over silica gel indicator. Yield: 0.222 g (75%). Anal. calcd. (found) % for $C_6H_{20}N_{10}Cu$ (**1**): C, 24.36 (24.58); H, 6.81 (6.72); N, 47.35 (47.25). IR (KBr, cm^{-1}): $\nu_{asy}(N_3)$ 2020; $\nu_s(N_3)$ 1340. UV-Vis [MeCN; λ_{max}/nm (ε_{max}/dm^3 $mol^{-1}cm^{-1}$]: 265, 290 (1.25×10^4), 386 (1.10×10^4), 611 (2.25×10^2). Λ_M (MeCN): 7 Ω^{-1} cm^2 mol^{-1}.

Synthesis of $[Cu(TMEDA)(\mu_{1,1}\text{-}N_3)(N_3)]_2$ (2): The ligand *viz*. TMEDA (0.074 g, 1 mmol) was added to methanolic solution (20 mL) of copper(II) chloride dihydrate (0.170 g, 1 mmol). To this mixture, sodium azide (0.130 g, 2 mmol) in MeOH (15 mL) was added slowly with constant stirring. The final deep green solution was filtered and the supernatant liquid was kept undisturbed in open air for slow evaporation. After a weak blue crystalline product **2** was isolated by filtration, washed with dihydrated alcohol and dried *in vacuo* over silica gel. Yield: 0.266 g (60%). Anal. calcd. (found) % for $C_6H_{20}N_{16}Cu_2$ (**2**): C, 16.25 (16.34); H, 4.55 (4.68); N, 31.59 (31.70): $\nu_{asy}(N_3)$ 2054, 2031; $\nu_s(N_3)$ 1330, 1345. UV-Vis [MeCN; λ_{max}/nm (ε_{max}/dm^3 $mol^{-1}cm^{-1}$]: 267, 298 (1.25×10^4), 389 (1.10×10^4), 612 (2.25×10^2). Λ_M (MeCN): 8 , Ω^{-1} cm^2 mol^{-1}.

X-ray data collection and structure refinement: Single crystals of complexes **1** and **2** suitable for X-ray analysis were selected from those obtained by slow evaporation of a methanolic solution at room temperature. Diffraction data were collected on a Bruker SMART 1000 CCD diffractometer using graphite monochro-mated MoKα radiation (λ = 0.71073 Å) and used to measure cell dimensions and diffraction intensities. The ω-θ scan technique were applied to collect data in the range to a maximum $2.7° < \theta < 25.5°$. For data collection, data reduction and cell refinement the program SAINT-Plus [29] was used. The structure was solved by direct methods using SIR97 [30] and refined with version 2018/3 of SHELXL [31] using least squares minimization. The amine H atoms were located on a difference Fourier map and refined freely. The C-bound H atoms were positioned geometrically and refined using a riding model, with C-H = 0.96-0.97 Å and with Uiso = 1.2 Ueq(C) or 1.5 Ueq(C) for methyl H atoms. The final positional and thermal parameters are available as supplementary material. A summary of the crystallographic data and structure determination parameters for complexes **1** and **2** is set in Table-1. Selected bond distances and bond angles relevant to the metal coordination spheres are given in Table-2. Hydrogen bond interaction parameters are shown in Table-3.

RESULTS AND DISCUSSION

Two neutral copper(II) azido complexes of the types mononuclear $[Cu(TMEDA)_2(N_3)_2]$ (**1**) and dinuclear $[Cu(TMEDA)(\mu_{1,1}\text{-}N_3)(N_3)]_2$ (**2**) [TMEDA = trimethylenediamine; N_3^- = azide ion] have been isolated using one-pot reaction of a 1:2:2/1:1:2

TABLE-1
CRYSTALLOGRAPHIC DATA FOR COMPLEXES **1** AND **2**

	Complex **1**	Complex **2**
Empirical formula	$C_6H_{20}N_{10}Cu$	$C_6H_{20}N_{16}Cu_2$
Formula weight	295.86	443.46
Crystal system, space group	Triclinic, *P*-1	Monoclinic, $P2_1/n$
Temperature	293(2) K	293(2) K
Wavelength	0.71073 Å	0.71073 Å
Unit cell dimensions	a = 6.6977(10) Å, b = 6.7826(10) Å, c = 8.2537(12) Å, α = 93.358(2)°, β = 98.456(2)°, γ = 119.2662(18)°	a = 6.873(2)Å, b = 6.780(2) Å, c = 18.446(5) Å, α = 90°, β = 99.653(4)°, γ = 90°
Volume	319.81(8) Å^3	847.4(4) Å^3
Z, calculated density	2, 3.072 mg/cm^3	4, 1.738 mg/cm^3
Absorption coefficient	3.413 mm^{-1}	2.538 mm^{-1}
F(000)	310	1412
Crystal size	0.21 × 0.15 × 0.09 mm^3	0.25 × 0.18 × 0.14 mm^3
θ range	2.52 to 26.29°	2.24 to 25.25°
Limiting indices	-8<=h<=8, -8<=k<=8, -10<=l<=10	-8<=h<=8, -8<=k<=8, -22<=l<=22
Reflections collected/unique	3867/1307 [R(int) = 0.019]	8090/1525 [R(int) = 0.055]
T_{max} and T_{min}	0.612 and 0.514	0.644 and 0.522
Data/restraints/parameters	1307/0/79	1525/0/109
Goodness-of-fit on F^2	1.083	1.072
Final R indices [I>2σ(I)]	R = 0.0242 and *w*R = 0.0657	R = 0.1156 and *w*R = 0.3425
R indices (all data)	R = 0.0247 and *w*R = 0.0659	R = 0.1181 and *w*R = 0.3436
Largest peak and hole	0.486 and -0.208 eÅ^{-3}	2.821 and -1.793 eÅ^{-3}

Weighting scheme: $R = \Sigma||F_o| - |F_c||/\Sigma|F_o|$, $wR = [\Sigma w(F_o^2 - F_c^2)^2/\Sigma w(F_o^2)^2]^{1/2}$, calcd $w = 1/[\sigma^2(F_o^2) + (xP)^2 + yP]$; x = 0.0397, y = 0.0804 for **1**; x = 0.1357, y = 0.7924 for **2**, where $P = (F_o^2 + 2F_c^2)/3$

TABLE-2
SELECTED BOND DISTANCES (Å) AND BOND ANGLES (°) FOR COMPLEXES **1** AND **2**

Compound **1**			
Bond distances			
Cu1-N1	2.0354(19)	Cu1-N3	2.6800(2)
Cu1-N2	2.0324(2)	Cu1-N3^i	2.6800(2)
Cu1-N1^i	2.0354(19)	N3-N4	1.170(2)
Cu1-N2^i	2.0324(2)	N4-N5	1.168(2)
Bond angles			
N1-Cu1-N2	87.15(6)	N2-Cu1-N3^1	87.16(11)
N1-Cu1-N3	87.16(11)	N1^i-Cu1-N3	92.84(11)
N1-Cu1-N1^i	180.00(11)	N2^i-Cu1-N3	96.16(7)
N1-Cu1-N2^i	92.85(6)	N2-Cu1-N2^i	180.00(13)
N1-Cu1-N3^i	92.84(7)	N3-Cu1-N3^i	180.00(11)
N2-Cu1-N3	83.84(7)	N2^i-Cu1-N3^i	83.84(7)
N1^i-Cu1-N2	92.85(6)	N3-N4-N5	179.8(2)
N2-Cu1-N2^i	180.00(13)		
Symmetry code: (i) -x, -y, -z			

Compound **2**			
Bond distances			
Cu1-N1	1.990(13)	N3-N4	1.162(17)
Cu1-N2	1.991(12)	N4-N5	1.17(2)
Cu1-N3	2.022(13)	N6-N7	1.214(18)
Cu1-N6	2.006(14)	N7-N8	1.136(18)
Cu1-N3^i	2.464(13)	Cu1-Cu1^i	3.327(2)
Bond angles			
N1-Cu1-N2	95.8(5)	N2-Cu1-N3^i	94.4(5)
N1-Cu1-N3	84.5(5)	N3-Cu1-N6	92.6(5)
N1-Cu1-N6	174.7(5)	N3-Cu1-N3^i	84.8(5)
N1-Cu1-N3^i	90.9(5)	Cu1-N3-Cu1^i	95.2(5)
N2-Cu1-N3	179.1(5)	N3-N4-N5	175.1(19)
N2-Cu1-N6	87.8(6)	N6-N7-N8	179.3(16)
Symmetry code: (i) = 1-x,-y,1-z			

TABLE-3
HYDROGEN BOND INTERACTION PARAMETERS (Å, °) FOR COMPLEXES **1** AND **2**

Complex	D–H···A	D–H	H···A	D···A	D–H···A	Symmetry code
1	N1–H1A···N5	0.9000	2.0800	2.969(3)	172.00	1–x,–y,–z
	N1–H2A···N5	0.9000	2.3700	3.227(3)	158.00	1–x,1–y,–z
	N2–H2B···N5	0.9000	2.2400	2.083(3)	156.00	–1+x,y,z
	C3–H3A···N4	0.9700	2.6200	2.382(3)	135.00	–x,–y,–z
2	N1–H1A···N8	0.9000	2.3300	3.20(2)	164.00	–x,–y,1–z
	N1–H1B···N6	0.9000	2.4900	3.348(19)	160.00	1–x,–y,1–z
	N2–H2A···N6	0.9000	2.2400	3.106(18)	160.00	1–x,1–y,1–z
	N2–H2B···N8	0.9000	2.2300	3.09(2)	160.00	–x,1–y,1–z
	C2–H2D···N8	0.9700	2.5800	2.46(3)	152.00	1/2+x,1/2–y,1/2+z

molar ratios of $CuCl_2 \cdot 2H_2O$, TMEDA and NaN_3 in methanol at room temperature. The typical syntheses are summarized in **Scheme-II**. Complexes (**1** and **2**) were characterized by microanalytical, spectroscopic and other physico-chemical results. The microanalytical data are in good conformity with the formulation. The air stable mois-ture insensitive compounds are stable over long periods of time in powdery and crystalline states and are soluble in MeOH, EtOH, MeCN, DMF and DMSO, but are insoluble in water. In MeCN solutions, complexes **1** and **2** behave as non-electro-lytes as reflected in their low conductivity values (~7 Ω^{-1} cm^2 mol^{-1}).

IR and electronic spectra: The IR spectra of complexes **1** and **2** were recorded in KBr discs in 4400-400 cm^{-1} region. The varied types of metal-azido linkages [32] in the IR spectrum of complex **1** were assigned due to the presence of two strong absorption bands at 2040 and 2018 cm^{-1} associated with $\nu_{asy}(N_3)$ stretching vibrations. Similarly, in complex **2**, the $\nu_{as(N_3)}$ stretching vibrations appeared at 2054 and 2031 cm^{-1}, respectively. The medium intensity absorption band at ~1340 cm^{-1} for both the complexes are the indicative of $\nu_s(N_3)$ stretching vibrations. The electronic spectra of complexes **1** and **2** have been measured in MeCN solutions in the 200-900 nm range [33]. A weak low-intensity absorption band at ~610 nm is assignable to *d-d* transition, consistent with the square pyramidal (*sp*) geometry of the copper(II) centers [34]. The absorption band observed at ~380 nm may be attributed to the ligand to copper(II) charge transfer transition (LMCT) [35]. Additionally, two strong absorption bands in the region ~265 and ~295 nm may be assigned to a ligand-based charge transfer transitions [35].

Crystal structure of $[Cu(TMEDA)_2(N_3)_2]$ (1): In order to define the coordination spheres of $[Cu(TMEDA)_2(N_3)_2]$ (**1**), single-crystal X-ray diffraction measurements was made. The $[Cu(TMEDA)_2(N_3)_2]$ (**1**) crystal belongs to the triclinic system corresponding from the space group P-1, which is recognized as centro-symmetric system. An ORTEP diagram of molecular unit in $[Cu(TMEDA)_2(N_3)_2]$ (**1**) is depicted in Fig. 1 and 2D supramolecular sheet structure in Fig. 2. Single crystal X-ray diffraction measurement of complex **1** revealed that each Cu(II) center in complex **1** assumes an octahedral geometry with a CuN_6 chromophore coordinated by the four N atoms (N1, N2, N1^i and N2^i) of two different TMEDA ligands as bidentate chelator and two N atoms (N3, N3^i) of two terminal azide ions [symmetry code: (i) -x, -y, -z] (Fig. 1). The equatorial positions are occupied by four N atoms (N1, N2, N1^1 and N2^i) while another two N atoms (N3 and N3^i) are placed in the axial positions. Distortion from ideal octahedral geometry is presumably due to the smaller bite angle N2-Cu1-N3 83.84(7)º and N2^i-Cu1-N3^i 83.84(7)º in complex **1** created at the metal center. The degree of distortion from an ideal octahedral geometry has been reflected in the *cisoid* [83.84(7)º-96.16(7)º] and the *transoid* [180.00(11)º-180.00(13)º] bond angles. The Cu-N distances are ranging from 2.0324(2)-2.6800(2) Å (Table-2). Here the pair (Cu1-N1; Cu1-N1^i)/(Cu1-N2; Cu1-N2^i)/(Cu1-N3; Cu1-N3^i) is identical in length. The Cu-N_{azide} bond lengths [Cu1-N3/Cu1-N3^i 2.6800(2) Å] are longer compare to other Cu-N_{ligand} bond lengths [Cu1-N1/Cu1-N1^i 2.0354(19) Å and Cu1-N2/Cu1-N2^i 2.0324(2) Å]. Each metal(II) center deviates 0.035 Å from the mean basal plane. The propylenic part (N1-C1-C2-C3-N2) of the symmetrical amine is to some extent puckered. The terminal azide ions in metal bound state are in linear fashion as reflected in the bond angles [N3-N4-N5/N3^i-N4^i-N5^i 179.8(2)º]. In the crystalline state of **1**, mononuclear units are engaged in intermolecular N-H···N (N1-H1A···N5: 2.0800 Å, 172.00º; N1-H2A···N5: 2.3700 Å, 158.00°; N2-H2B···N5: 2.2400 Å, 156.00º) and C-H···N (C3-H3A···N4: 2.6200 Å, 135.00º) hydrogen bonds (Table-3) by participation of H atoms (H1A/H2A/H2B/H3A) of -NH_2 groups of chelator TMEDA as the donor and N atoms (N4/N5) of terminal azide

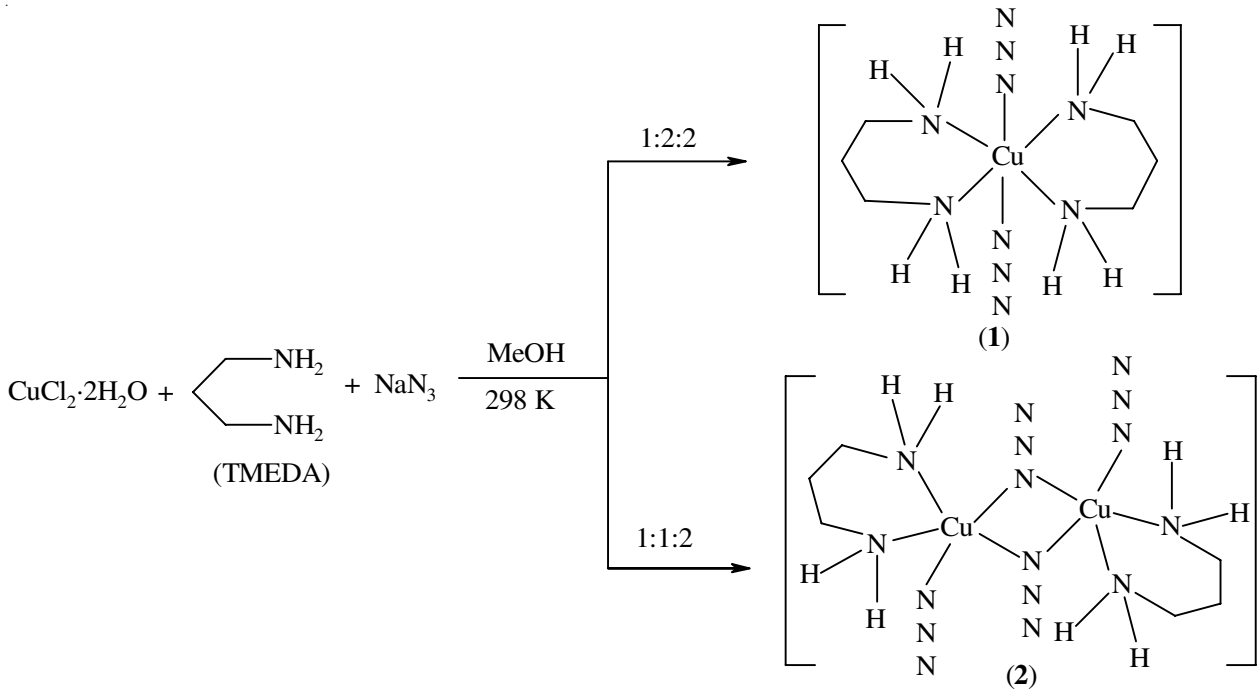

Scheme-II. Synthetic route for complexes **1** and **2**

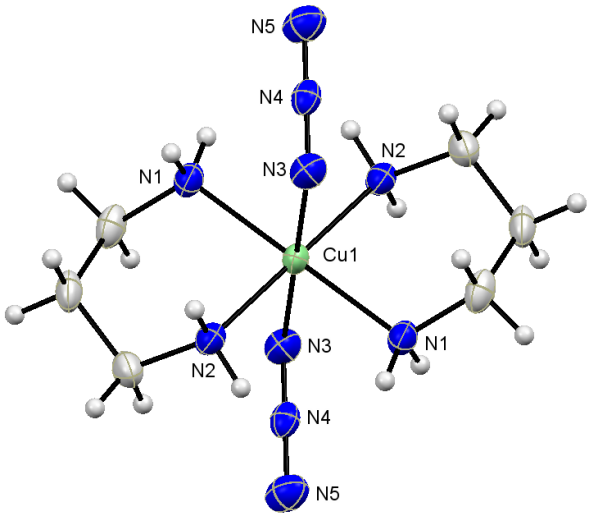

Fig. 1. An ORTEP diagram of molecular unit of **1** with displacement ellipsoids drawn at the 40% probability level [Symmetry code: (i) -x, -y, -z]

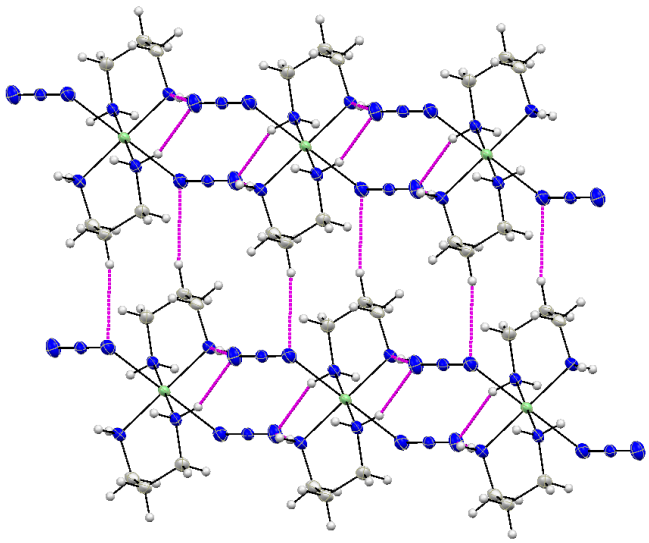

Fig. 2. Packing diagram of 2D sheet structure in **1** through intermolecular N–H···N and C–H···N hydrogen bonds viewed along the *b* axis

ions as acceptor affording a supramolecular 3D network structure (Fig. 2).

Crystal structure of [Cu(TMEDA)($\mu_{1,1}$-N_3)(N_3)]$_2$ (2): Single-crystal X-ray diffraction measurement of [Cu(TMEDA)-($\mu_{1,1}$-N_3)(N_3)]$_2$ (**2**) reveals that the crystal belongs to the monoclinic system corresponding from the space group P21/n. An ORTEP diagram of and packing image of 2D and 3D super structures of complex **2** are presented in Figs. 3-5, respectively. The coordination sphere around each Cu center in the complex **2**, can best be stated as a distorted square pyramidal geometry (t = 0.073) having a CuN_5 chromophore [36] coordinated through two N atoms (N1, N2) of TMEDA as bidentate chelator, one N atom (N3) of bridging azide ($\mu_{1,1}$-N_3) and one N atom (N6) of terminal azide forming the basal plane and one N atom [N3^i; symmetry code (i) = 1-x,-y,1-z] of another bridging azide ($\mu_{1,1}$-N_3) occupying the apical position (Fig. 3). The centrosymmetric dinuclear unit was formed between two copper centers

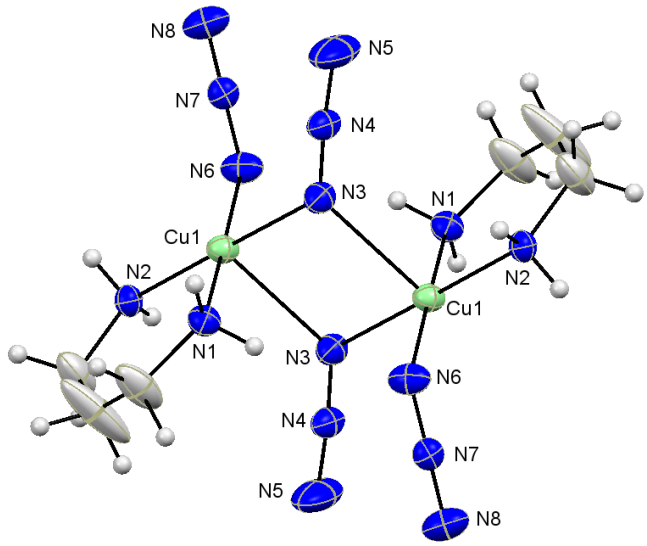

Fig. 3. An ORTEP diagram of molecular unit of **2** with displacement ellipsoids drawn at the 30% probability level

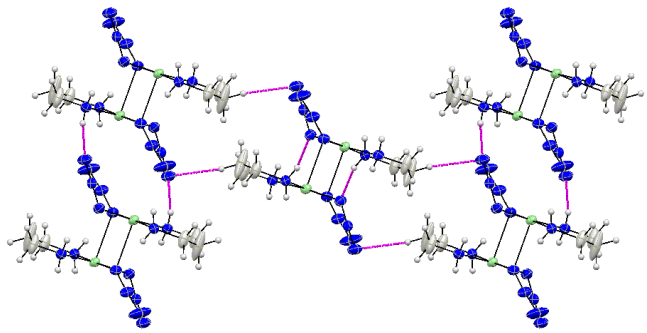

Fig. 4. Packing view of supramolecular 2D sheet structure in **2** through intermolecular N–H···N hydrogen bonds viewed along the *b* axis

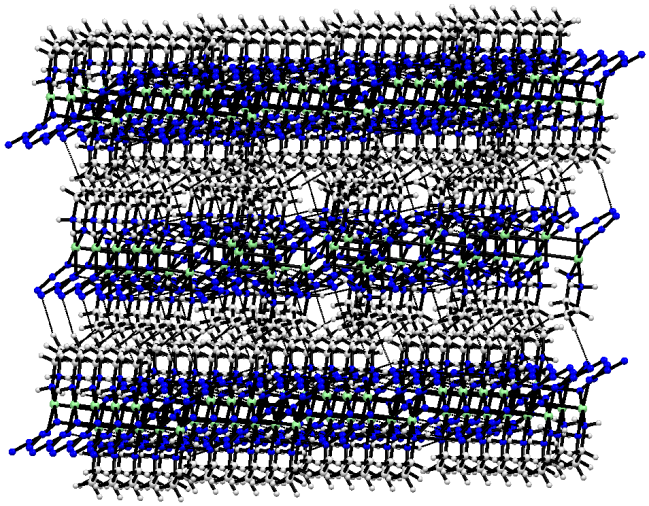

Fig. 5. Packing view of supramolecular 3D network structure in **2** through intermolecular N–H···N and C–H···N hydrogen bonds viewed along the *b* axis

through double μ_2-$_{1,1}$-N_3 bridges. The Cu···Cu separation in dinuclear unit is 3.327(2) Å. The equatorial Cu-N distances [1.990(13)-2.022(13) Å] are somehow reduced than apical Cu-N distance [2.464(13) Å] (Table-2). The Cu1 metal is

displaced by 0.0981(19) Å from the basal plane towards the apical $N3^{i}$ atom. The Cu1-$N3^{i}$ line forms a dihedral angle of 8.91(5)° with the normal to the mean basal plane. The geometry of the centrosymmetric dimeric complex molecule formed by bridging role of the N3-N4-N5 azide anions could be described in terms of square pyramids sharing a base-to-apex edge with parallel basal planes; the dihedral angle between the basal planes of the copper centers in the dinuclear unit is 0° by symmetry, whereas the Cu_2N_2 core forms a dihedral angle of 92.2(5)º with each basal plane. The propylenic part (N1-C1-C2-C3-N2) of the symmetrical amine is to some extent puckered. In the crystalline state, the dimeric units in complex **2** are associated through intermolecular N-H···N (N1-H1A ···N8: 2.3300 Å, 164.00°; N1-H1B···N6: 2.4900 Å, 160.00º; N2-H2A···N6: 2.2400 Å, 160.00°; N2-H2B···N8: 2.2300 Å, 160.00°) hydrogen bonds between the N atoms of terminal azide ions (N6/N8) with H atoms (H1A/H1B/H2A/H2B) of amine hydrogen of TMEDA ligand (Table-3) to afford a 2D sheet structure along the crystallographic *b*-axis (Fig. 4). These 2D sheet structure is further stabilized by C-H···N hydrogen bonds [C2-H2D···N8: 2.5800 Å, 152.00º] between the N atom of terminal azide ion (N8) with H atoms (H2D) of TMEDA to form 3D network architecture (Fig. 5) in complex **2**.

Magnetic study of [Cu(TMEDA)($\mu_{1,1}$-N_3)(N_3)]$_2$ (2): Variable temperature magnetic susceptibility measurement of complex **2** has been measured on a powdered monocrystalline sample in the temperature range 2-300 K under the external magnetic field of 0.5 T. The temperature dependence of χ_M of complex **2** is shown in Fig. 6. Upon cooling χ_M remains almost constant up to around 50 K and then rapidly increases with temperature. The χ_M at room temperature, 1.25×10^{-3} cm^3 mol^{-1} is comparable with spin-only value of 1.25×10^{-3} cm^3 mol^{-1} expected for an isolated copper(II) ions (S = ½) assuming g = 2.00. The fitting of $1/\chi_M$ *versus T* plot with the Curie-Weiss equation affords C = 0.37 emu mol^{-1} K and θ = -22.23 K for complex **2** (Fig. 7). This clearly indicates that a moderate antiferromagnetic interaction between copper(II) ions is operative in the dimer moiety of complex **2**. To estimate the magnitude of the antiferromagnetic coupling the magnetic susceptibility

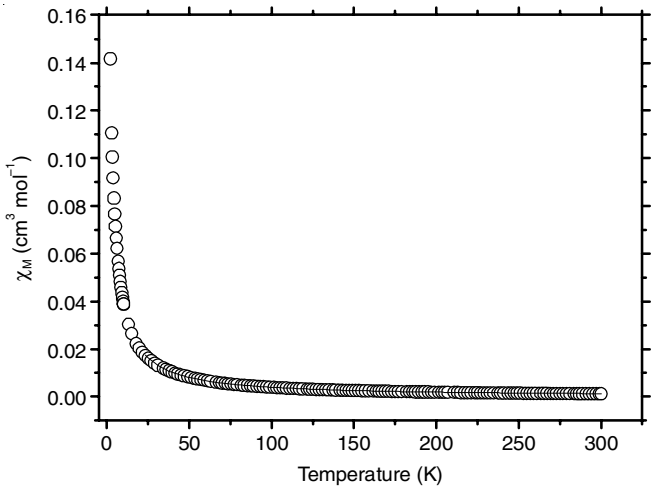

Fig. 6. Plot of χ_MT *versus* T (%) for complex **2**; solid lines represent the best fit of the data with the model described in the text

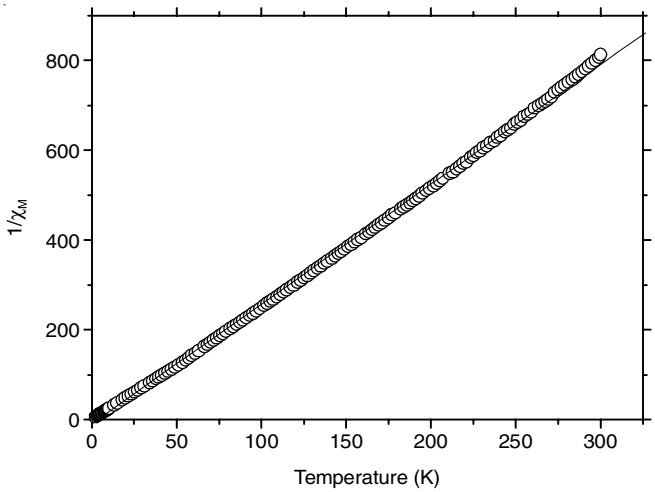

Fig. 7. Plot of $1/\chi_M$ *versus* T (%) for complex **2**; solid lines represent the best fit of the data with the model described in the text

data (300-3K) were fitted to the modified Bleaney-Bowers equation [37] for two interacting copper(II) ions (S = ½) with the Hamiltonian in the form $H = -J\hat{S}_1 \cdot \hat{S}_2$. The susceptibility equation for such a dimeric system can be written as follows:

$$\chi = \frac{2Ng^2\beta^2}{kT}\left[3 + \exp\left(-\frac{J}{kT}\right)\right]^{-1}(1-\rho) + \frac{Ng^2\beta^2}{2kT}\rho$$

where N, g, β and ρ parameters in the equation bear their usual meaning. Fitting of the magnetic susceptibility data up to 23 K with the equation (1) yielded the parameter values J = -0.40 cm^{-1}, g = 2.3(1), with an agreement factor $R = 1.9 \times 10^{-8}$.

Antibacterial activity: A comparative account of the growth inhibition zone values of ligand (TMEDA) and their corresponding complexes **1** and **2** revealed that azido complexes showed higher antibacterial activity than the free ligand as represented in Table-4. This is probably due to the greater lipophilic nature of the complexes. Such increased activity of the metal chelates can be explained on the basis of Overtone's concept and Tweedy's chelation theory [38]. According to Overtone's concept of cell permeability, the lipid membrane that surrounds the cell favours the passage of only lipid soluble materials due to which liposolubility is considered to be an important factor that controls the anti microbial activity. On chelation, the polarity of the metal ion will be reduced to a greater extent due to the overlap of the ligand orbital and partial sharing of the positive charge of the metal ion with donor groups [39,40]. Further, it increases the delocalization of the π-electrons over the whole chelate ring and enhances the lipophilicity of the complex. This increased lipophilicity enhances the penetration of the complexes into lipid membrane and thus blocks the metal binding sites on enzymes of microorganisms [41]. These metal complexes also disturb the respiration process of the cell and thus block the synthesis of proteins, which restricts further growth of the organism [42]. The variation in the activity of different complexes against different organisms depend either on the impermeability of the cells of the microbes or difference in ribosomes of microbial cells. The inhibition zones of antibacterial activity are presented in Table-4.

TABLE-4
GROWTH INHIBITION ZONE (mm) OF MICROBES

Microbes	Ligand TMEDA	Complex $[Cu(TMEDA)_2(N_3)_2]$ (**1**)	Complex $[Cu(TMEDA)(\mu_{1,1}\text{-}N_3)(N_3)]_2$ (**2**)
E. coli	7	12	9
S. aureus	5	12	13
A. niger	15	22	18
F. oxysporum	11	15	16

Conclusion

In summary, complexes **1** and **2** are the illustrations of the versatility of the azido bridge for building molecular based materials. Structural analysis revealed that each copper(II) center in mononuclear **1** adopts an octahedral geometry with a CuN_6 chromophore. The structure of complex **1** is stabilized by intermolecular N-H···N and C-H···N hydrogen bonds interactions forming a 2D sheet structure. In complex **2**, each Cu(II) center is in a distorted square pyramidal geometry with CuN_5 chromophore, which is linked to each other by double μ_2-$_{1,1}$-azido bridges to form dinuclear unit. These dinuclear units are further associated with intermolecular N-H···N and C-H···N hydrogen bonds to form a 3D network structure. The variable-temperature magnetic susceptibility measurements revealed weak antiferromagnetic coupling between the metal centers in complex **2** through double $\mu_{1,1}$-azido bridges. The preparation of such compounds illustrates a potentially versatile approach towards construction of uncharged metal-organic frameworks. Biological studies indicate that better activity was found for the complexes when compared to that against their corresponding ligand.

ACKNOWLEDGEMENTS

The work is financially supported by the Department of Science and Technology, Government of India, by a grant (SR/S1/IC-0013/2010).

CONFLICT OF INTEREST

The authors declare that there is no conflict of interests regarding the publication of this article.

REFERENCES

1. R. Ricco, C. Pfeiffer, K. Sumida, C.J. Sumby, P. Falcaro, S. Furukawa, N.R. Champness and C.J. Doonan, *CrystEngComm*, **18**, 6532 (2016); https://doi.org/10.1039/C6CE01030J
2. R.R. Ozer and J.P. Hinestroza, *RSC Adv.*, **5**, 15198 (2015); https://doi.org/10.1039/C4RA15161E
3. T. N. Mandal, A. Karmakar, S. Sharma and S.K. Ghosh, *Chem. Record*, **18**, 154 (2018); https://doi.org/10.1002/tcr.201700033
4. Z.N. Wang, X. Wang, S. Yue Wei, J. Xiao Wang, F. Ying Bai, Y. Heng Xing and L. Xian Sun, *New J. Chem.*, **39**, 4168 (2015); https://doi.org/10.1039/C5NJ00173K
5. C. Mottillo and T. Friscic, *Chem. Commun.*, **51**, 8924 (2015); https://doi.org/10.1039/C5CC01645B
6. R. Chakrabarty, P.S. Mukherjee and P.J. Stang, *Chem. Rev.*, **111**, 6810 (2011); https://doi.org/10.1021/cr200077m
7. M.L. Neidig, D.L. Clark and R.L. Martin, *Coord. Chem. Rev.*, **257**, 394 (2013); https://doi.org/10.1016/j.ccr.2012.04.029
8. J. Reedijk, *Chem. Soc. Rev.*, **42**, 1776 (2013); https://doi.org/10.1039/C2CS35239G
9. R.D. Willet, D. Gatteschi and O. Kahn, eds., Magneto-Structural Correlations in Exchange Coupled Systems, NATO ASI Series: Reidel, Dordrecht (1985).
10. M.M. Turnbull, T. Sugimoto and L.K. Thompson, Molecular Based Magnetic Materials: Theory, Techniques and Applications, ACS Symposium Series, no. 644, ACS: Washington (1996).
11. A. Caneschi, D. Gatteschi, L. Pardi and R. Sessoli, ed.: A.F. Williams Clusters, Chains and Layered Molecules: The Chemists Way to Magnetic Materials, In: Perspectives in Coordination Chemistry, VCH: Weinheim (1992).
12. J.L. Manson, A.M. Arif and J.S. Miller, *Chem. Commun.*, 1479 (1999); https://doi.org/10.1039/a903406d
13. O. Kahn, *Condens. Mater. Phys*, **17**, 39 (1994).
14. J.R. Long, ed.: P. Yang, Molecular Cluster Magnets in Chemistry of Nanostructured Materials: World Scientific: Hong Kong (2003).
15. L.K. Thompson and S.K. Tandon, *Comments Inorg. Chem.*, **18**, 125 (1996); https://doi.org/10.1080/02603599608032718
16. A. Escuer and G. Aromí, *Eur. J. Inorg. Chem.*, **2006**, 4721 (2006); https://doi.org/10.1002/ejic.200600552
17. Y.-F. Zeng, X. Hu, F.-C. Liu and X.-H. Bu, *Chem. Soc. Rev.*, **38**, 469 (2009); https://doi.org/10.1039/B718581M
18. S. Saha, D. Mal, S. Koner, A. Bhattacherjee, P. Gütlich, S. Mondal, M. Mukherjee and K.-I. Okamoto, *Polyhedron*, **23**, 1811 (2004); https://doi.org/10.1016/j.poly.2004.04.007
19. J. Ribas, M. Monfort, I. Resino, B. Kumar Ghosh, X. Solans and M. Font-Bardia, *Polyhedron*, **17**, 1735 (1998); https://doi.org/10.1016/S0277-5387(97)00444-0
20. S. Koner, S. Iijima, M. Watanabe and M. Sato, *J. Coord. Chem.*, **56**, 103 (2003); https://doi.org/10.1080/0095897031000066060
21. N. Kuhn, T. Kratz, D. Bläser and R. Boese, *Adv. Inorg. Chem.*, **43**, 179 (1995); https://doi.org/10.1016/0020-1693(95)04701-A
22. R. Robson, *Aust. J. Chem.*, **23**, 2217 (1970); https://doi.org/10.1071/CH9702217c
23. A. Escuer, M.A.S. Goher, F.A. Mautner and R. Vicente, *Inorg. Chem.*, **39**, 2107 (2000); https://doi.org/10.1021/ic991135c
24. W.-W. Sun, X.-B. Qian, C.-Y. Tian and E.-Q. Gao, *Inorg. Chim. Acta*, **362**, 2744 (2009); https://doi.org/10.1016/j.ica.2008.12.016
25. B. Graham, M.T.W. Hearn, P.C. Junk, C.M. Kepert, F.E. Mabbs, B. Moubaraki, K.S. Murray and L. Spiccia, *Inorg. Chem.*, **40**, 1536 (2001); https://doi.org/10.1021/ic000991h
26. S. Youngme, T. Chotkhun, S. Leelasubcharoen, N. Chaichit, C. Pakawatchai, G.A. van Albada and J. Reedijk, *Polyhedron*, **26**, 725 (2007); https://doi.org/10.1016/j.poly.2006.09.073
27. J.D. Woodward, R.V. Backov, K.A. Abboud, D. Dai, H.-J. Koo, M.-H. Whangbo, M.W. Meisel and D.R. Talham, *Inorg. Chem.*, **44**, 638 (2005); https://doi.org/10.1021/ic049175q
28. E.A. Boudreaux and L.N. Mulay, Theory and Applications of Molecular Paramagnetism, Wiley-Interscience: New York (1976).
29. Bruker APEX2, (Version 2008.1-0), SAINT (Version 7.51A) and SADABS (Version 2007/4) Bruker AXS Inc. Madison, Wisconsin: USA (2008).

30. A. Altomare, M.C. Burla, M. Camalli, G.L. Cascarano, C. Giacovazzo, A. Guagliardi, A.G.G. Moliterni, G. Polidori and R. Spagna, *J. Appl. Cryst.*, **32**, 115 (1999); https://doi.org/10.1107/S0021889898007717
31. G.M. Sheldrick, *Acta Crystallogr. C*, **71**, 3 (2015); https://doi.org/10.1107/S2053229614024218
32. K. Nakamoto, Infrared and Raman Spectra of Inorganic and Coordination Compounds, Part A and B, Wiley: NewYork, edn 5 (1997).
33. A.B.P. Lever, Inorganic Electronic Spectroscopy, Elsevier: New York, edn 2 (1984).
34. P. Dapporto, M. Formica, V. Fusi, L. Giorgi, M. Micheloni, P. Paoli, R. Pontellini and P. Rossi, *Inorg. Chem.*, **40**, 6186 (2001); https://doi.org/10.1021/ic0105415
35. T. Gajda, A. Jancsó, S. Mikkola, H. Lönnberg and H. Sirges, *J. Chem. Soc., Dalton Trans.*, 1757 (2002); https://doi.org/10.1039/b108948j
36. A.W. Addison, T.N. Rao, J. Reedijk, J. van Rijn and G.C. Verschoor, *J. Chem. Soc., Dalton Trans.*, 1349 (1984); https://doi.org/10.1039/DT9840001349
37. O. Kahn, Molecular Magnetism, VCH: New York (1993).
38. B.G. Tweedy, *Phytopathology*, **55**, 910 (1964).
39. K. Kralova, K. Kissova, O. Svajlenova and J. Vanco, *Chem. Pap.*, **58**, 361 (2000).
40. J. Parekh, P. Inamdhar, R. Nair, S. Baluja and S. Chanda, *J. Serb. Chem. Soc.*, **70**, 1155 (2005); https://doi.org/10.2298/JSC0510155P
41. Y. Vaghasiya, R. Nair, M. Soni, S. Baluja and S. Shanda, *J. Serb. Chem. Soc.*, **69**, 991 (2004); https://doi.org/10.2298/JSC0412991V
42. N. Raman, *Res. J. Chem. Environ.*, **4**, 9 (2005).